Making 2-D Materials Mechanochemically by Twin-Screw Extrusion

Chen, Haili; Cao, Qun; Ye, Ziwei; Lai, Beibei; Zhang, Yuancheng; Dong, He; Crawford, Deborah E.; Istrate, Oana M.; James, Stuart L.

DOI:
10.1002/admt.202301780

ADVANCED MATERIALS TECHNOLOGIES
www.advmattechnol.de

Making 2-D Materials Mechanochemically by Twin-Screw Extrusion: Continuous Exfoliation of Graphite to Multi-Layered Graphene

Haili Chen, Qun Cao, Ziwei Ye, Beibei Lai, Yuancheng Zhang, He Dong, Deborah E. Crawford, Oana M. Istrate, and Stuart L. James**

Mechanochemistry has developed rapidly in recent years for efficient chemicals and materials synthesis. Twin screw extrusion (TSE) is a particularly promising technique in this regard because of its continuous and scalable nature. A key aspect of TSE is that it provides high shear and mixing. Because of the high shear, it potentially also offers a way to delaminate 2-D materials. Indeed, the synthesis of 2-D materials in a scalable and continuous manor remains a challenge in their industrialization. Here, as a proof-of-principle, the automated, continuous mechanochemical exfoliation of graphite to give multi-layer graphene (MLG, ≈6 layers) by TSE is demonstrated. To achieve this, a solid-and-liquid-assisted extrusion (SLAE) process is developed in which organic additives such as pyrene are rendered liquid due to the high temperatures used, to assist with the exfoliation, and simultaneously solid sodium chloride is used as a grinding aid. This gave MLG in high yield (25 wt%) with a short residence time (8 min) and notably with negligible evidence for structural deterioration (defects or oxidation).

1. Introduction

Mechanochemistry is emerging as an effective and powerful tool for chemical and materials synthesis.[1] Reactive extrusion has emerged as a promising approach for transitioning mechanochemistry from batch operation methods like ball-milling to scalable and continuous "flow" processes. Its applicability has been demonstrated in the fields of co-crystallization,[2] metal–organic frameworks (MOFs) and porous cage synthesis,[3] sustainable organic synthesis,[4] and deep eutectic solvent production.[5] The most common approach is to use twin screw extrusion (TSE). In TSE, reactant material is conveyed by two rotating screws along a tightly-fitting barrel which imparts high shear and mixing forces to the reactants. In 2019, reactive extrusion was highlighted by International Union of Pure and Applied Chemistry (IUPAC) as one of the ten most important chemical innovations that could change our world.[6] Given the growing applicability of reactive extrusion to synthesis, and the fact that it provides high shear forces,[7] we were motivated to explore the potential for exfoliation of 2-D materials using this technique. This is of particular interest because the economical production of 2-D materials in a scalable continuous manor remains a challenge.

H. Chen
College of Chemistry and Materials Engineering
Zhejiang A&F University
Hangzhou 311300, P. R. China

H. Chen, Q. Cao, Z. Ye, B. Lai, Y. Zhang, H. Dong, D. E. Crawford, S. L. James
School of Chemistry and Chemical Engineering
Queen's University Belfast
David Keir Building, Stranmillis Rd., Belfast BT9 5AG, UK
E-mail: qc52@le.ac.uk; s.james@qub.ac.uk

Y. Zhang
MOF Technologies
Belfast BT7 1NF, UK

D. E. Crawford
School of Chemistry
University of Birmingham
Edgbaston, Birmingham BT15 2TT, UK

O. M. Istrate
School of Mechanical and Aerospace Engineering
Queen's University Belfast
Ashby Building, Stranmillis Rd. Belfast, Belfast BT9 5AG, UK

The ORCID identification number(s) for the author(s) of this article can be found under https://doi.org/10.1002/admt.202301780

DOI: 10.1002/admt.202301780

As one of the best-known 2-D nanomaterials, graphene has gained widespread interest due to its outstanding mechanical, optical, and electronic properties, and promise for applications.[8] Several methods for the mechanical exfoliation of graphite to graphene have been developed, including sonication,[9] high-shear mixing techniques[10] (e.g., spinning disc reactors[10c] and vortex fluidic devices[10d–f]), as well as ball-milling.[11] However, many of these forementioned techniques have drawbacks including long exfoliation times, low yields, the requirement for large quantities of solvents for graphene stabilization and industrial-scale controllability.[12] Within the last decade, there have been numerous successful demonstrations of producing 2-D materials such as MoS_2, MXene, BN, and graphene oxide under continuous flow conditions using vortex fluidic exfoliation.[13] Compared to batch processes, continuous processes can potentially offer advantages such as consistent product quality, lower labor during operation and enhanced process safety.[14] Numerous attempts have been made to transition the exfoliation of graphite to graphene from batch mode to continuous flow manufacturing. For instance, methods such as vortex fluidic exfoliation[10d–f] three-roll milling[15] and internal-circular sonication[16] have been explored. However, due to the extended exfoliation time needed (ranging from 0.5 h to up to 16 h), these techniques were still predominantly operated under batch mode. To our knowledge, there is no existing continuous flow mechanical exfoliation process for production of graphene from graphite.

Extrusion processes can provide a well-controlled reaction environment (e.g., stable reaction temperature, steady specific mechanical energy input, constant feeding and production rates) and are scalable. Herein, we investigate the possibility of producing 2-D materials by continuous exfoliation using twin-screw extruder, with graphene as proof-of-concept example.

2. Results and Discussion

Previous studies have shown that graphite can be exfoliated to single- or few-layered graphene in high yields under ball-milling conditions in the presence of organic additives (e.g., melamine,[17] triazine derivatives,[18] pyrene[19] or 4-hydroxybenoic acid[20]) as protective diluents. It was proposed that during the dry-milling graphite exfoliation process solid organic additives could not only act as grinding aids to transfer mechanical forces from the extruder to the graphite, but also compete with the van der Waals attraction between the graphite layers, thus aiding in the exfoliation process.[17,21] Additionally, inorganic salts like NaCl, $CsCl_2$ as well as silica gel, have been employed as grinding auxiliaries to enhance grinding efficiency during ball milling or TSE.[22] These studies provided a starting point for our work. In particular, graphite powder and solid additives (e.g., NaCl in conjunction with biphenyl, pyrene, naphthene, melamine or 4-hydroxybenzoic acid) were first mixed in a 1:28 weight ratio. This mixture was fed manually into the extruder at room temperature over a 20 min period through the feeding port (ca. ≈0.8 g min^{-1}) using a screw rotation rate of 100 rpm, which resulted in a residence time of ca. 15 min and an average torque of ≈2.2 Nm (**Figure 1a**). The solid extrudate was collected and the remaining additives were fully removed by washing with suitable solvents (Section S2.1, Supporting Information). The carbonaceous product was analyzed by thermogravimetric analysis (TGA) and scanning electron microscopy (SEM) to screen for conversion to graphene. Regev and co-workers demonstrated the utility of TGA in characterizing the structural parameters (mean lateral dimension, polydispersity) of graphene-based materials.[23] Based on the literature and the TGA data we obtained, the following parameters were extracted: 1) the mean combustion temperature $T_{1/2}$ (the temperature of the combustion step at which half of the total weight loss has occurred – an indicator of the particle size/thickness), 2) the combustion temperature range ΔT (the temperature range within which the graphene sheets combust, determined as the difference between the lower and upper onset temperatures – an indicator of polydispersity). An example of how ΔT and $T_{1/2}$ were extracted from the TGA of graphite is shown in Figure S1a (Supporting Information). The extracted ΔT and $T_{1/2}$ parameters were then plotted as ΔT versus $T_{1/2}$ to give a thermal phase diagram (TPD) (Figure 1b, for details of TGA analysis method see Section 3.1, Supporting Information). It has been described that TGA parameters characteristic of various carbon materials occur in distinct temperature ranges in their TPDs. For instance, amorphous carbon exhibited a $T_{1/2}$ value typically in the range of 400–500 °C, while for graphene materials (e.g., few layer graphene, multi-layered graphene, and graphene nanoplates) it occurs in the 575–750 °C range.[19,23] As shown in Figure 1b, extrusion of graphite in the presence of only organic solids (e.g., biphenyl, pyrene, naphthene, 4-HBC, melamine) led to a decrease of $T_{1/2}$ from 770 °C (graphite) to 700–750 °C and an increase of ΔT from 200 °C to up to 231 °C, indicating that a degree of exfoliation had occurred during extrusion, albeit resulting in materials with high polydispersity. Extrusion in the presence of only an inorganic salt (e.g., NaCl) as additive decreased the particle size, thickness and polydispersity the obtained crude graphene material further ($T_{1/2}$ = 620 °C, ΔT = 180 °C). Unfortunately, extrusion in the presence of both pyrene and NaCl as additives (or with a lower NaCl content in the feed mixture, graphite: NaCl = 1: 14) led to greater polydispersity (ΔT > 220 °C) and a lower degree of exfoliation ($T_{1/2}$ > 630 °C), and increasing the NaCl content in the feed mixture (graphite: NaCl = 1: 56) did not significantly improve these characteristics. As mentioned above, the TPDs of a variety of commercial carbon-based materials as well as graphene exfoliated by ball milling have been studied by Regev and co-workers[19,20,23] with the $T_{1/2}$ values for graphene materials (e.g., few layer graphene, multi-layered graphene, and graphene nanoplates) found to occur between 575 and 750 °C. Although the $T_{1/2}$ of carbonaceous products obtained by extrusion with solid additives shown in Figure 1b fall within this range (specifically 610–750 °C), SEM images of these materials indicated that large amounts of unexfoliated graphite remained (Figure S2b, Supporting Information) in the product, in accordance with their high ΔT values (>180 °C).

Various organic additives such as dimethylformamide (DMF),[24] 1-pyrene carboxylic acid,[25] *N*-methyl-2-pyrrolidone (NMP),[26] ionic liquids,[27] and deep eutectic solvents[28] have been employed as exfoliants due to their ability to prevent re-aggregation of delaminated graphene sheets and reduce structural damage, ascribed to their strong hydrogen bonding, π–π or cation-π based interactions.[21b,29] It has also been reported that the addition of small amounts of solvent during the milling process can facilitate the intercalation of solid exfoliants

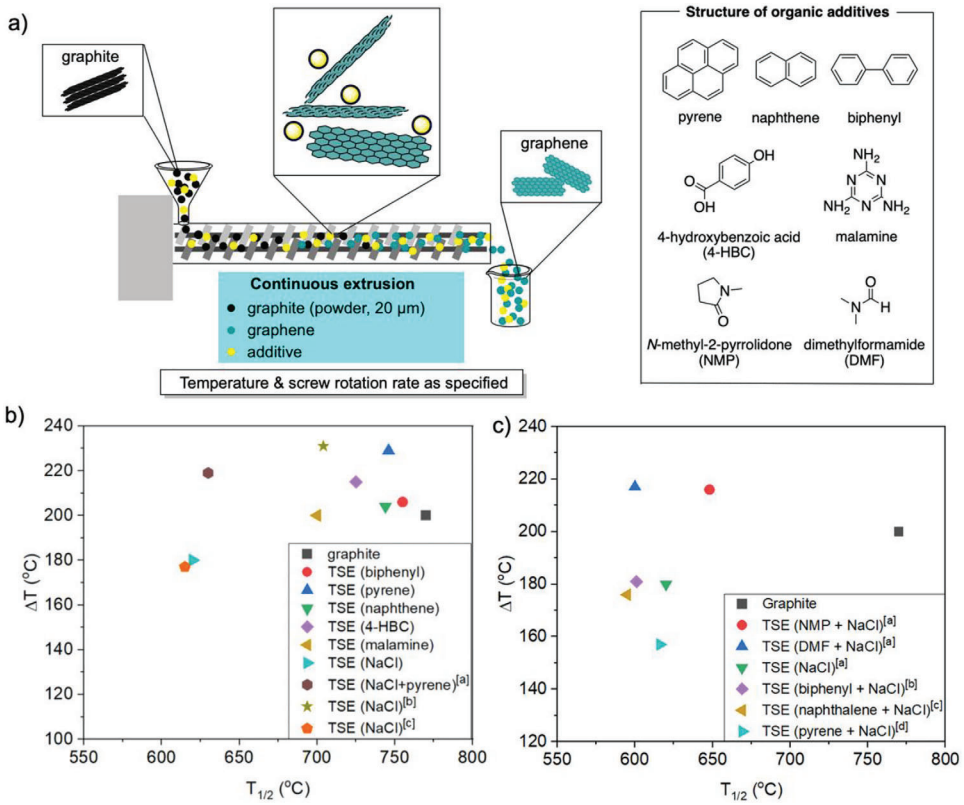

Figure 1. Continuous exfoliation of graphite to graphene with various additives. a) cartoon of exfoliation of graphite to graphene using TSE and structures of organic additives. b) ΔT versus $T_{1/2}$ thermal phase diagram of products obtained by extrusion at room temperature (graphite: additives = 1: 28 (w/w), feeding rate = 0.8 g min^{-1}, screw rotation rate = 100 rpm, torque = 1.8–2.5 Nm). [a] graphite: NaCl: pyrene = 1: 28: 7, [b] graphite: NaCl = 1:14, [c] graphite: NaCl = 1:56. c) ΔT versus $T_{1/2}$ thermal phase diagram of products obtained with various additives under liquid assisted extrusion conditions (graphite: NaCl: organic additive = 1:56:10 (w/w/w), feeding rate = 0.8 g min^{-1}, rotation rate = 200 rpm at specified temperature). [a] room temperature, [b] 70 °C, [c] 80 °C, [d] 160 °C.

(e.g., melamine) between the graphite layers, and promote greater exfoliation.[30] Inspired by those findings, we explored the effect of having both solid and liquid phases present to assist in the extrusion process. In particular, NMP or DMF were used as the liquid exfoliation aid and NaCl as a physical solid grinding aid. The liquid additive was added via syringe pump to maintain a weight ratio of graphite: NaCl: organic additive of 1:56:10 (feeding rate = 0.8 g min^{-1}, screw rotation rate = 200 rpm, average torque = 1.8–2.5 Nm). However, these experiments led to limited exfoliation as indicated by ΔT for the products being greater than 210 °C (Figure 1c). It is possible that these liquids provided lubrication within the extruder barrel which lowered the shear force exerted on the material, and may not be ideal as exfoliation aids. However, a helpful feature of TSE (and which is not standard in commercial ball mills) is that the barrel can be heated and maintained at a stable temperature during the extrusion process. Therefore, in order to maintain the potential for π–π stacking interaction between the polyaromatic exfoliating agents and graphite, while simultaneously promoting diffusion of the organic species between the graphite layers, extrusion in the presence of these organic additives (e.g., pyrene, biphenyl or naphthalene) was investigated by applying temperatures greater than the melting point of the organic additive (Figure 1c). After being fed into the extruder at the elevated temperature, the solid organic additive should melt, whereas NaCl should continue to act as a solid grinding auxiliary to deliver shearing forces during extrusion and enable effective exfoliation. Interestingly, it was notable that under these semi-melt conditions, a dramatic increase in torque to 5–9 Nm occurred during extrusion, suggesting that greater shear was being applied to the material in the extruder barrel. Correspondingly, compared to the material obtained by extrusion with NaCl as sole additive, this high temperature solid-and-liquid-assisted-extrusion (SLAE) process yielded materials with markedly lower $T_{1/2}$ values (i.e., 595–616 °C). The experimental findings indicated the ΔT of the carbon materials obtained using the aforementioned additives followed the order $\Delta T_{NaCl} > \Delta T_{NaCl+naphthene} > \Delta T_{NaCl+pyrene}$. Perhaps significantly, this trend closely resembled that for ΔT values of carbon materials obtained under dry ball milling conditions.[19] Thus, it is postulated that the low $T_{1/2}$ and ΔT values are attributed to both the elevated torque imparted by SLAE conditions and the effective chemical interactions between the melted organic additives and carbon materials. Under the optimized SLAE conditions (graphite: NaCl: pyrene = 1:56:10 (w/w/w)), with a feeding rate = 0.8 g min^{-1} and screw rotation rate of 200 rpm) at 160 °C, the resulted carbon material exhibited the lowest ΔT value of 157 °C. Subsequently, this material was used further characterization (for representative TGA and

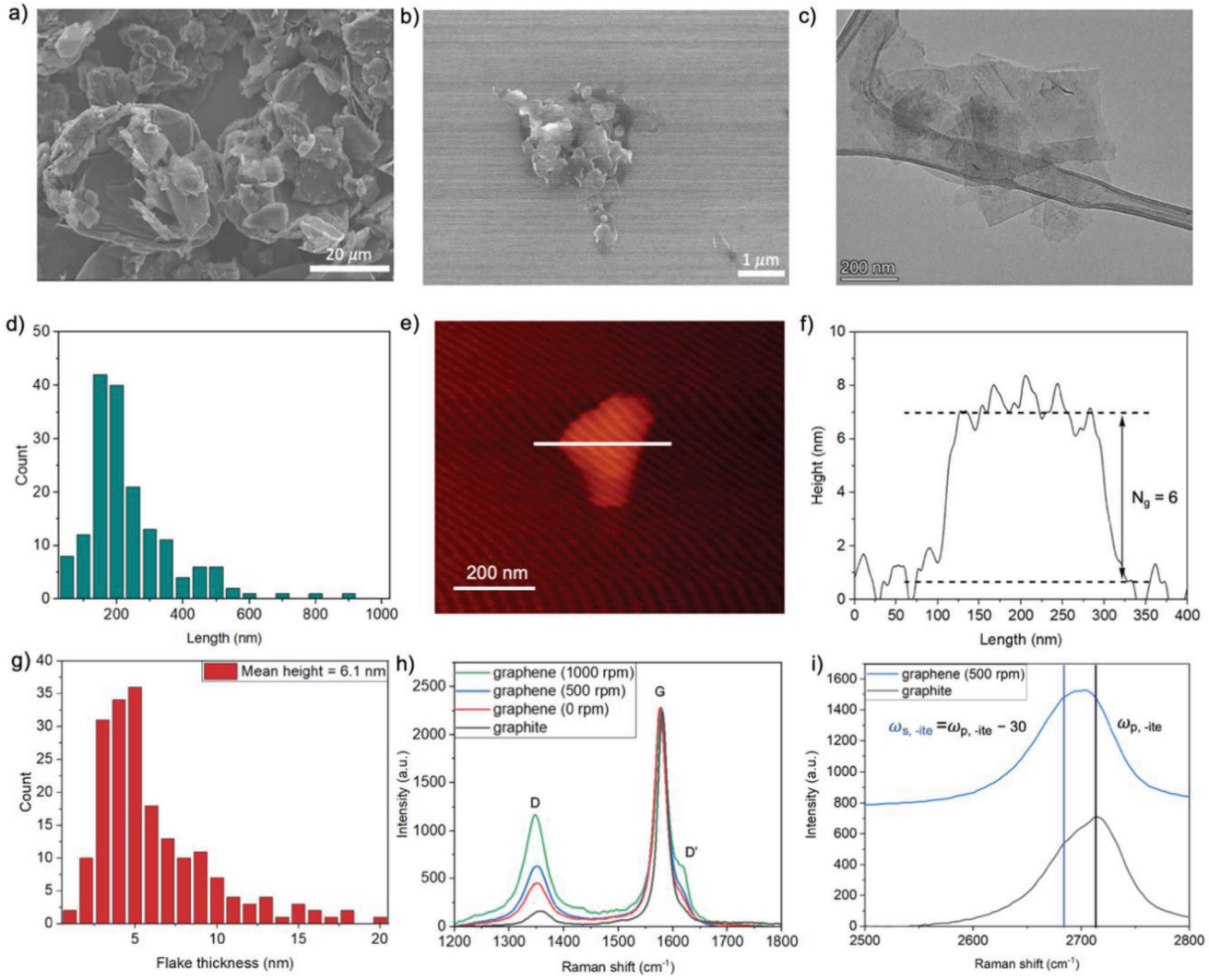

Figure 2. Characterization of graphite and graphene sheets. a) SEM image of graphite powder (Sigma Aldrich, 20 μm). b) Representative SEM image of multi-layered graphene obtained by centrifuge of crude graphene sheets. c) Representative TEM image of exfoliated graphene sheets. d) Length distribution of extrusion exfoliated graphene as measured from TEM images of 170 flakes. e,f) Representative AFM image of multi-layered graphene and corresponding height profiles. g) Representative AFM height histogram for extrusion exfoliated multi-layered graphene. h) Raman spectra of extrusion exfoliated graphene with the increase of centrifugation speed. i) Raman spectra of 2D band for raw graphite and extrusion exfoliated graphene.

derivative thermogravimetry (DTG) data see Figure S1b, Supporting Information).

It has been reported that graphite exfoliated by prolonged ball milling (>6 h) in air suffers from oxidation, to give graphene oxide.[31] However, according to X-ray photoelectron spectroscopy (XPS), the surface of the pyrene-NaCl exfoliated crude graphene was similar to that of the raw graphite material, indicating that negligible oxidation had occurred under these extrusion conditions (Figure S5, Supporting Information). This may relate to the short residence time (ca. 8 min) compared to several hours needed for exfoliation by ball milling, as well as the lack of high-energy impact forces that can occur during milling. SEM showed that while the graphite before extrusion consisted mainly of particles in the size range 10–50 μm (**Figure 2**a; Figure S2a, Supporting Information), the crude graphene sheets obtained by SLAE with pyrene and NaCl had an average lateral size of <1 μm, albeit together with some unexfoliated graphite (Figure S2c, Supporting Information). Further analysis by TGA (Figure S1, Supporting Information), energy dispersive X-ray spectroscopy (EDS, Figures S3 and S4, Supporting Information) analyses revealed the absence of residual additives (e.g., pyrene, NaCl or Fe) in the crude graphene sheets. XPS analysis of Cl2p (Figure S6, Supporting Information) revealed that the crude graphene product was not contaminated by chloride from NaCl (or was below detection limit of XPS). To remove the unexfoliated graphite, the material was dispersed in NMP (1 mg mL^{-1}), sonicated for 5 min, then centrifuged at 500 rpm (centrifugation force 42 g) for 45 min (for SEM image of graphene sheets after centrifugation see Figure 2b and Figure S2d, Supporting Information).[10a,26]

Through carefully repeated transmission electron microscopy (TEM) verification, it was discovered that the NMP supernatant did not contain any large graphitic particles but did contain

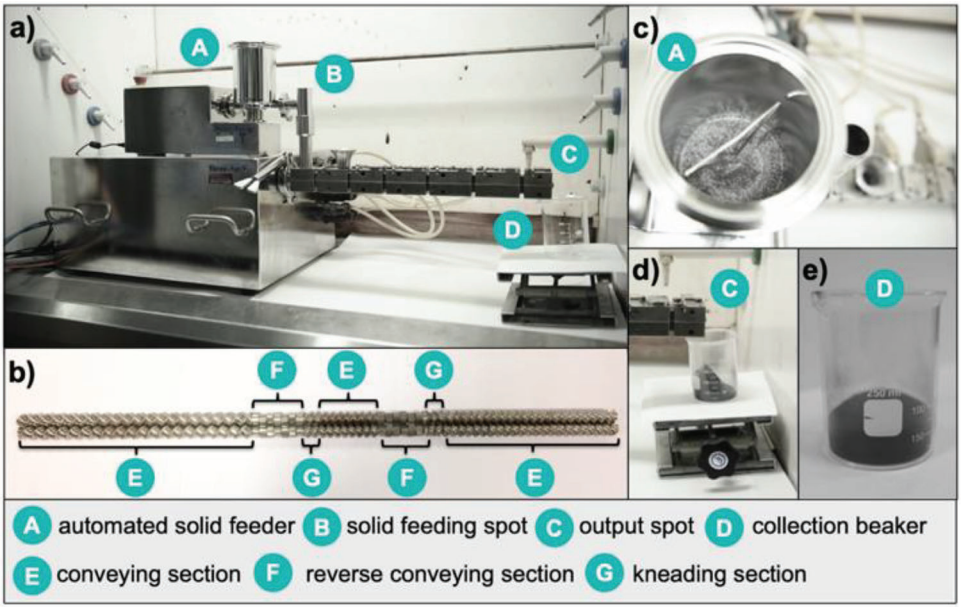

Figure 3. Automated continuous TSE process for manufacturing graphene from graphite. a) overview of TSE with automated solid feeder; b) image of extruder screw with reverse conveying section; c) automated solid feeder with graphite: NaCl: pyrene = 1:56:10 (w/w/w), feeding rate = 0.8 g min^{-1}, rotation rate = 200 rpm at 160 °C; d,e) mixed material after extrusion.

graphene sheets (for representative TEM images of graphene sheets see Figure 2c; Figure S7a-d,g, Supporting Information). To characterize their lateral size, statistical length analysis was performed by TEM as summarized in the histogram in Figure 2d. The results show lateral size in the range 50–800 nm with most particles (≈80%) lying between 150 and 400 nm. In addition, their corresponding selected area electron diffraction (SAED) (Figure S7e,h, Supporting Information) presented a hexagonal pattern indicating undamaged in-plane structure. The diffraction intensities from the (0-110) and (1-210) planes indicated that both multi-layer and monolayer sheets were present (Figure S7d-i, Supporting Information).[32] The stable graphene suspension obtained after centrifugation (500 rpm, 42 g, 45 min) was also imaged by atomic force microscopy (AFM) for statistical height analysis of 190 particles (Figure 2e,f; Figure S8, Supporting Information). This gave an average thickness of 6.1 nm and indicated that the majority could be classified as multi-layer graphene (taken to be 5–10 layers,[33] consistent with the generally accepted premise that the height of a single graphene sheet layer should be taken as ≈1 nm in AFM analysis[10a]). Raman spectroscopic analysis was carried out to analyze the defect density (through the relative intensities of the D and G bands, I_D/I_G) and defect types (through $I_D/I_{D'}$) as well as the number of graphene layers present (through the position of the 2D bands), as shown in Figure 2h,i, respectively (see Figure S9, Supporting Information for representative Raman spectra). The I_D/I_G ratio increased from 0.04 for the untreated graphite to up to 0.52 for material obtained with increasing centrifugation speed (from 0 to 1000 rpm, equivalent to 0 –168 g) indicating that the remaining flakes became smaller. The values of $I_D/I_{D'}$ for products obtained at different centrifugation speeds were in the range 1.6–1.8, which, being less than 7, suggests that the optimized extrusion process did not introduce vacancy-like defects into the basal plane of the graphene produced.[34] This is in good agreement with the XPS data (Figure S5, Supporting Information) in which the similar values of %sp^3 hybridized carbons (e.g., C–C, C–H, C–O) were obtained from graphite (≈17%) and the crude graphene sheets (≈18%). A formula proposed by Coleman and co-workers[10a] relates the average number of layers to the 2D Raman band through the empirical relation $NG = 10^{0.84M+0.45M^2}$, where the metric M is given by

$$M = \frac{I_{2D\text{-ene}}\left(\omega = \omega_{p(-ite)}\right)/I_{2D\text{-ene}}\left(\omega = \omega_{s(-ite)}\right)}{I_{2D\text{-ite}}\left(\omega = \omega_{p(-ite)}\right)/I_{2D\text{-ite}}\left(\omega = \omega_{s(-ite)}\right)} \quad (1)$$

in which $I_{2D\text{-ene}}$ and $I_{2D\text{-ite}}$ are the intensities of the 2D bands for graphene and graphite respectively (see Figure 2i; Section 3.6, Supporting Information for details). This gave the average number of layers as 6.9, in good agreement with the values obtained from the AFM analysis.

With AFM, TEM and Raman data showing that multi-layer graphene could be produced from graphite by TSE, a continuous TSE process was set up with automated reagent feed via a volumetric solid feeder. Under the optimized conditions, a solid mixture of graphite, NaCl and pyrene in 1:56: 10 weight ratio was fed into the preheated extruder barrel (160 °C) at 0.8 g min^{-1} over 1 h with a screw rotation rate of 200 rpm (**Figure 3** and the video file in the Supporting Information). A grey crude solid extrudate was collected from 18 to 60 min.

The extrudate was washed with acetone and water repeatedly, whereupon the pyrene precipitated and could thereby be recycled via filtration (for the recycle procedure see Section 2.2, Supporting Information). The recycled pyrene was analyzed by LC-MS and compared with pure pyrene (Figure S10, Supporting Information), revealing no chlorinated pyrene in the samples. The extrudate was collected by filtration and dried in an oven to give

≈0.5 g crude graphene sheets. Some of this crude material (0.1 g) was dispersed in NMP (100 mL) and centrifuged at 500 rpm (42 g) for 45 min to give 0.0245 g multi-layer graphene. This yield of 25 wt% is eight times greater than that reported for a high shear mixing process (3.35 wt%).[9b] The bulk electric conductivity of the multi-layered graphene was measured using Four-Point Probe Measurement, yielding values of ≈4.5 × 10^3 Sm^{-1} at 10 MPa (thickness of 1.1 mm) and ≈1 × 10^4 Sm^{-1} at 30 MPa (thickness of 0.77 mm). These findings were consistent with previously reported literature, where the conductivity of few-layer graphene or multi-layer graphene was reported in the order of 10^3–10^4 Sm^{-1}.[10a,15,24,35] It can be noted that the extruder used in this study is a relatively small research instrument (screw diameter 11 mm, 40:1 L/D ratio). The specific mechanical energy (SME) during this TSE process supplied to the mixture by continuous extrusion was calculated to be only ≈13.5 kJ g^{-1} using the equation:

$$SME = \frac{P_{motor}}{\tau_{max} \times N_{max}} \times \frac{\tau \times N}{Q} \quad (2)$$

where P_{motor} is the maximum motor power (460 W), τ is the drive motor torque (τ_{max} = 12 Nm, τ = ≈7 Nm), N is the screw rotation rate (N_{max} = 300 rpm, N = 200 rpm) and Q is the feeding rate (0.8 g min^{-1}).[36] However, even at a feeding rate of only 48 g h^{-1} and SME of 13.5 kJ g^{-1}, a throughput rate of 4.3 g day^{-1} (0.18 g h^{-1}) multi-layer graphene, could in principle be obtained from graphite powder, which is 2–20 times greater than for the reported ball-milling processes (see Section S4, Tables S2 and S3 and Figures S12 and S13 for further comparation). Based on the yield of multi-layer graphene during twin-screw extrusion (TSE) at 25 wt% and the theoretically calculated milling energy required to exfoliate and fragment graphite into ≈0.3 µm graphene sheets (0.145 kJ g^{-1}, detailed in the Supporting Information), the efficiency of the supplied specific mechanical energy (SME) is ≈0.004% with an E-factor of 4842 (detailed calculation see Section S5, Supporting Information). This efficiency is lower than the previously reported ball-milling efficiencies, which typically range from 0.1% to 1%.[19,37]

Efforts were undertaken to utilize pristine graphite obtained from Sigma Aldrich, which was characterized by an average particle size larger than >500 µm. However, minimal amounts of multi-layered graphene were obtained under the current optimized exfoliation conditions, likely due to the limited SME in the continuous process during the short residence time. Industrial grade extruders, which are widely available, are normally equipped with more powerful motors (e.g., 6000 kW),[38] indicating the potential for enhancing production rates, yields and the utilization of larger graphite as starting material with such equipment.

3. Conclusion

We have developed a rapid (≈8 min residence time), efficient (25 wt% yield) and potentially scalable continuous flow process for exfoliation of graphite to MLG (average number of layers ≈6) by TSE. The method relies on the simultaneous use of both liquid and solid additives to assist in the exfoliation process. We suggest that the liquid arene is able to diffuse into the material and stabilise exfoliated sheets while the solid additive acts as a physical grinding aid. As a continuous flow mechanical exfoliation process, this method allows the fast production (0.18 g h^{-1}) of relatively large quantities of multi-layer graphene with negligible structural deterioration (e.g., defects or oxidation), in both regards showing advantages over ball milling. Although the produced graphene may not reach few- or single-layered quality at a production rate comparable to industrialized high shear exfoliation in liquid systems,[10a] these findings are significant in demonstrating the feasibility and efficacy of TSE for 2-D material synthesis. We noted that in its current form the process results in waste NaCl, pyrene and solvents and that minimisation of this waste is an important point for further development. The application of this approach to the exfoliation of other layered materials is currently under investigation.

4. Experimental Section

Materials: Carbon materials: Graphite (powder, 20 µm, synthetic, CAS: 7782-42-5) was purchased from Sigma Aldrich. Additives: NaCl (CAS 7647-14-5) was purchased from Glacia (food grade pure dried vacuum salt). Pyrene (CAS: 129-00-0), naphthalene (CAS: 91-20-3), biphenyl (CAS: 92-52-4), 4-hydroxybenzoic acid (CAS: 99-96-7), *N*-methyl-2-pyrrolidone (CAS: 872-50-4), *N*,*N*-dimethylformamide (CAS: 68-12-2), melamine (CAS: 108-78-1) were purchased from Sigma Aldrich. Pyrene, naphthalene, biphenyl and 4-hydroxybenzoic acid were ground before use to give smooth powders, all the other materials were used as received.

Twin Screw Extruder: The continuous extrusion of graphite to graphene was carried out using a co-rotating twin screw extruder manufactured by Three-Tec with a screw diameter of 12 mm, a length to diameter ratio of 40:1 and six heating zones. The screw rotation rate of the twin screw extruder could be varied from 25 to 300 rpm and the temperature can be increased from ambient to 300 °C. For extrusion above ambient temperature, all six heating zones were heated to the same temperature. The volumetric twin-screw solid feeder (ZD 9 FB) was purchased from Three-Tec. The free volume of the extruder barrel (without screws) was 4.83 × 10^{-3} m^3.

Automated Continuous Exfoliation of Graphite to Graphene by Twin-Screw Extruder: A pre-mixed mixture of graphite (1.62 g), sodium chloride (90 g) and pyrene powder (15 g) was poured into the volumetric twin-screw feeder. The addition rate was adjusted to ≈0.8 g min^{-1} (graphite = ≈12.2 mg min^{-1}) by setting the feed rate of the feeder to 8%. The screw rotation rate was 200 rpm and the extruder barrel was heated to 160 °C. After ≈8 min the reaction mixture smoothly exited the barrel as grey powder. After a further 10 min, the torque of the extruder stabilized between 5 and 9 Nm. A 250 mL glass beaker was used to collect the extrudate. After running the exfoliation process for 40 min, ≈32 g extrudate had been collected. The extrudate was washed with water (3 × 100 mL) and acetone (3 × 100 mL), collected by filtration and dried at 110 °C overnight in an oven to give crude graphene sheets (0.49 g). The crude graphene sheets were analyzed by Raman Spectroscopy, TGA, XPS, SEM.

Supporting Information

Supporting Information is available from the Wiley Online Library or from the author.

Acknowledgements

This work was supported by the EPSRC Impact Acceleration Account funding (IAA1718-01-0618, IAA1718-04-1117), EPSRC funding (EP/L019655/1) and Talent Start-up Project of Scientific Research and Development Foundation of Zhejiang A&F University (No. 2021FR008).

Conflict of Interest

The authors declare no conflict of interest.

Data Availability Statement

The data that support the findings of this study are available from the corresponding author upon reasonable request.

Keywords

2-D materials, continuous exfoliation, mechanochemistry, multi-layered graphene, twin-screw extrusion

Received: October 18, 2023
Revised: March 25, 2024
Published online:

[1] a) X. Liu, Y. Li, L. Zeng, X. Li, N. Chen, S. Bai, H. He, Q. Wang, C. Zhang, *Adv. Mater.* **2022**, *34*, 2108327; b) T. Friščić, C. Mottillo, H. M. Titi, *Angew. Chem., Int. Ed.* **2020**, *59*, 1018.

[2] a) D. Braga, L. Maini, F. Grepioni, *Chem. Soc. Rev.* **2013**, *42*, 7638; b) D. Douroumis, S. A. Ross, A. Nokhodchi, *Adv. Drug Del. Rev.* **2017**, *117*, 178.

[3] D. Crawford, J. Casaban, R. Haydon, N. Giri, T. McNally, S. L. James, *Chem. Sci.* **2015**, *6*, 1645.

[4] a) R. R. A. Bolt, J. A. Leitch, A. C. Jones, W. I. Nicholson, D. L. Browne, *Chem. Soc. Rev.* **2022**, *51*, 4243; b) Q. Cao, D. E. Crawford, C. Shi, S. L. James, *Angew. Chem., Int. Ed.* **2020**, *59*, 4478; c) D. E. Crawford, A. Porcheddu, A. S. McCalmont, F. Delogu, S. L. James, E. Colacino, *ACS Sustainable Chem. Eng.* **2020**, *8*, 12230; d) K. J. Ardila-Fierro, D. E. Crawford, A. Körner, S. L. James, C. Bolm, J. G. Hernández, *Green Chem.* **2018**, *20*, 1262; e) D. E. Crawford, C. K. G. Miskimmin, A. B. Albadarin, G. Walker, S. L. James, *Green Chem.* **2017**, *19*, 1507.

[5] D. E. Crawford, L. A. Wright, S. L. James, A. P. Abbott, *Chem. Commun.* **2016**, *52*, 4215.

[6] F. Gomollón-Bel, *Chem. Int.* **2019**, *41*, 12.

[7] a) M. J. Stevens, J. A. Covas, *Extruder Principles and Operation*, 2nd ed., Springer, Dordrecht **1995**; b) F. Lechner, in *Reactive Extrusion* (Eds: G. Beyer, C. Hopmann), Wiley-VCH, Weinheim, Germany **2017**, Ch. 2.

[8] a) A. C. Ferrari, F. Bonaccorso, V. Fal'ko, K. S. Novoselov, S. Roche, P. Bøggild, S. Borini, F. H. L. Koppens, V. Palermo, N. Pugno, J. A. Garrido, R. Sordan, A. Bianco, L. Ballerini, M. Prato, E. Lidorikis, J. Kivioja, C. Marinelli, T. Ryhänen, A. Morpurgo, J. N. Coleman, V. Nicolosi, L. Colombo, A. Fert, M. Garcia-Hernandez, A. Bachtold, G. F. Schneider, F. Guinea, C. Dekker, M. Barbone, et al., *Nanoscale* **2015**, *7*, 4598; b) V. Georgakilas, J. N. Tiwari, K. C. Kemp, J. A. Perman, A. B. Bourlinos, K. S. Kim, R. Zboril, *Chem. Rev.* **2016**, *116*, 5464; c) C. Tan, X. Cao, X.-J. Wu, Q. He, J. Yang, X. Zhang, J. Chen, W. Zhao, S. Han, G.-H. Nam, M. Sindoro, H. Zhang, *Chem. Rev.* **2017**, *117*, 6225.

[9] a) R. Hao, W. Qian, L. Zhang, Y. Hou, *Chem. Commun.* **2008**, 6576; b) Y. Hernandez, V. Nicolosi, M. Lotya, F. M. Blighe, Z. Sun, S. De, I. T. McGovern, B. Holland, M. Byrne, Y. K. Gun'Ko, J. J. Boland, P. Niraj, G. Duesberg, S. Krishnamurthy, R. Goodhue, J. Hutchison, V. Scardaci, A. C. Ferrari, J. N. Coleman, *Nat. Nanotechnol.* **2008**, *3*, 563; c) A. A. Green, M. C. Hersam, *Nano Lett.* **2009**, *9*, 4031; d) M. Lotya, Y. Hernandez, P. J. King, R. J. Smith, V. Nicolosi, L. S. Karlsson, F. M. Blighe, S. De, Z. Wang, I. T. McGovern, G. S. Duesberg, J. N. Coleman, *J. Am. Chem. Soc.* **2009**, *131*, 3611; e) U. Khan, A. O'Neill, M. Lotya, S. De, J. N. Coleman, *Small* **2010**, *6*, 864.

[10] a) K. R. Paton, E. Varrla, C. Backes, R. J. Smith, U. Khan, A. O'Neill, C. Boland, M. Lotya, O. M. Istrate, P. King, T. Higgins, S. Barwich, P. May, P. Puczkarski, I. Ahmed, M. Moebius, H. Pettersson, E. Long, J. Coelho, S. E. O'Brien, E. K. McGuire, B. M. Sanchez, G. S. Duesberg, N. McEvoy, T. J. Pennycook, C. Downing, A. Crossley, V. Nicolosi, J. N. Coleman, *Nat. Mater.* **2014**, *13*, 624; b) E. Varrla, K. R. Paton, C. Backes, A. Harvey, R. J. Smith, J. McCauley, J. N. Coleman, *Nanoscale* **2014**, *6*, 11810; c) J. Stafford, A. Patapas, N. Uzo, O. K. Matar, C. Petit, *AIChE J.* **2018**, *64*, 3246; d) X. Chen, J. F. Dobson, C. L. Raston, *Chem. Commun.* **2012**, *48*, 3703; e) M. H. Wahid, E. Eroglu, X. Chen, S. M. Smith, C. L. Raston, *Green Chem.* **2012**, *15*, 650; f) K. Vimalanathan, I. Suarez-Martinez, M. C. R. Peiris, J. Antonio, C. de Tomas, Y. Zou, J. Zou, X. Duan, R. N. Lamb, D. P. Harvey, T. M. D. Alharbi, C. T. Gibson, N. A. Marks, N. Darwish, C. L. Raston, *Nanoscale Adv* **2019**, *1*, 2495.

[11] a) M. I. Kairi, S. Dayou, N. I. Kairi, S. A. Bakar, B. Vigolo, A. R. Mohamed, *J. Mater. Chem. A* **2018**, *6*, 15010; b) M. Yi, Z. Shen, *J. Mater. Chem. A* **2015**, *3*, 11700.

[12] a) L. Lin, H. Peng, Z. Liu, *Nat. Mater.* **2019**, *18*, 520; b) K. S. Novoselov, V. I. Fal'ko, L. Colombo, P. R. Gellert, M. G. Schwab, K. Kim, *Nature* **2012**, *490*, 192; c) S. H. Choi, S. J. Yun, Y. S. Won, C. S. Oh, S. M. Kim, K. K. Kim, Y. H. Lee, *Nat. Commun.* **2022**, *13*, 1484.

[13] a) T. M. D. Alharbi, C. L. Raston, *Nanoscale Adv* **2023**, *5*, 6405; b) A. H. M. Al-antaki, S. Kellici, N. P. Power, W. D. Lawrance, C. L. Raston, *R. Soc. Open Sci.* **2020**, *7*, 192255; c) A. H. M. Al-Antaki, X. Luo, T. M. D. Alharbi, D. P. Harvey, S. Pye, J. Zou, W. Lawrance, C. L. Raston, *RSC Adv.* **2019**, *9*, 22074.

[14] a) R. Porta, M. Benaglia, A. Puglisi, *Org. Process Res. Dev.* **2016**, *20*, 2; b) G. Gambacorta, J. S. Sharley, I. R. Baxendale, *Beilstein J. Org. Chem.* **2021**, *17*, 1181; c) F. M. Akwi, P. Watts, *Chem. Commun.* **2018**, *54*, 13894.

[15] J. Chen, M. Duan, G. Chen, *J. Mater. Chem.* **2012**, *22*, 19625.

[16] M. Buzaglo, E. Ruse, I. Levy, R. Nadiv, G. Reuveni, M. Shtein, O. Regev, *Chem. Mater.* **2017**, *29*, 9998.

[17] a) V. León, M. Quintana, M. A. Herrero, J. L. G. Fierro, A. d. l. Hoz, M. Prato, E. Vázquez, *Chem. Commun.* **2011**, *47*, 10936; b) J. M. González-Domínguez, V. León, M. I. Lucío, M. Prato, E. Vázquez, *Nat. Protoc.* **2018**, *13*, 495.

[18] V. León, A. M. Rodriguez, P. Prieto, M. Prato, E. Vázquez, *ACS Nano* **2014**, *8*, 563.

[19] M. Buzaglo, I. P. Bar, M. Varenik, L. Shunak, S. Pevzner, O. Regev, *Adv. Mater.* **2017**, *29*, 1603528.

[20] E. Ruse, M. Buzaglo, I. Pri-Bar, L. Shunak, R. Nadiv, S. Pevzner, O. Siton-Mendelson, V. M. Skripnyuk, E. Rabkin, O. Regev, *Carbon* **2018**, *130*, 369.

[21] a) L. Liu, Z. Xiong, D. Hu, G. Wu, P. Chen, *Chem. Commun.* **2013**, *49*, 7890; b) J. D. Wuest, A. Rochefort, *Chem. Commun.* **2010**, *46*, 2923.

[22] a) Q. Cao, J. L. Howard, D. E. Crawford, S. L. James, D. L. Browne, *Green Chem.* **2018**, *20*, 4443; b) M. Leonardi, M. Villacampa, J. C. Menéndez, *Chem. Sci.* **2018**, *9*, 2042.

[23] M. Shtein, I. Pri-Bar, M. Varenik, O. Regev, *Anal. Chem.* **2015**, *87*, 4076.

[24] W. Zhao, M. Fang, F. Wu, H. Wu, L. Wang, G. Chen, *J. Mater. Chem.* **2010**, *20*, 5817.

[25] R. Aparna, N. Sivakumar, A. Balakrishnan, A. S. Nair, S. V. Nair, K. R. V. Subramanian, *J. Renew. Sustain. Energy* **2013**, *5*, 033123.

[26] C. Teng, D. Xie, J. Wang, Z. Yang, G. Ren, Y. Zhu, *Adv. Funct. Mater.* **2017**, *27*, 1700240.

[27] M. Matsumoto, Y. Saito, C. Park, T. Fukushima, T. Aida, *Nat. Chem.* **2015**, *7*, 730.

[28] A. M. Abdelkader, I. A. Kinloch, *ACS Sustainable Chem. Eng.* **2016**, *4*, 4465.

[29] a) R. Bari, G. Tamas, F. Irin, A. J. A. Aquino, M. J. Green, E. L. Quitevis, *Colloids Surf. A: Physicochem. Eng. Asp.* **2014**, *463*, 63; b) U. Patil, N. M. Caffrey, *J. Chem. Phys.* **2018**, *149*, 094702.
[30] A. E. Del Rio-Castillo, C. Merino, E. Díez-Barra, E. Vázquez, *Nano Res.* **2014**, *7*, 963.
[31] a) P. Dash, T. Dash, T. K. Rout, A. K. Sahu, S. K. Biswal, B. K. Mishra, *RSC Adv.* **2016**, *6*, 12657; b) A. E. D. Mahmoud, A. Stolle, M. Stelter, *ACS Sustainable Chem. Eng.* **2018**, *6*, 6358.
[32] a) J. C. Meyer, A. K. Geim, M. I. Katsnelson, K. S. Novoselov, D. Obergfell, S. Roth, C. Girit, A. Zettl, *Solid State Commun.* **2007**, *143*, 101; b) J. C. Meyer, A. K. Geim, M. I. Katsnelson, K. S. Novoselov, T. J. Booth, S. Roth, *Nature* **2007**, *446*, 60.
[33] A. Bianco, H.-M. Cheng, T. Enoki, Y. Gogotsi, R. H. Hurt, N. Koratkar, T. Kyotani, M. Monthioux, C. R. Park, J. M. D. Tascon, J. Zhang, *Carbon* **2013**, *65*, 1.
[34] A. Eckmann, A. Felten, A. Mishchenko, L. Britnell, R. Krupke, K. S. Novoselov, C. Casiraghi, *Nano Lett.* **2012**, *12*, 3925.
[35] B. Marinho, M. Ghislandi, E. Tkalya, C. E. Koning, G. de With, *Powder Technol.* **2012**, *221*, 351.
[36] S. Godavarti, M. V. Karwe, *J. Agric. Eng. Res.* **1997**, *67*, 277.
[37] D. W. Fuerstenau, A. Z. M. Abouzeid, *Int. J. Miner. Process.* **2002**, *67*, 161.
[38] Motors for extruders, https://www.menzel-motors.com/extruder-drive/ (accessed: August 2023).